Optical and Optoelectronic Studies of Binary and Ternary Films of Poly(L-Tryptophane), Poly(5-hydroxy-L-tryptophane), and P(TER-CO-TRI) Doped with Sudan Dye

Barham K. Rahim[1], Peshawa O. Amin[2], Fahmi F. Muhammadsharif[3], Salah R. Saeed[4], and Kamal A. Ketuly[5]

[1]Department of Medical Physics, Faculty of Medicals and Applied Science, Charmo University, 46023 Chamchamal, Sulaimania, Kurdistan Region - F.R. Iraq

[2]Charmo Center for Research, Training and Consultancy, Charmo University, 46023 Chamchamal, Kurdistan Region - F.R Iraq

[3]Department of Physics, Faculty of Science and Health, Koya University, 44023 Koya, Kurdistan Region - F.R Iraq

[4]Department of Physics, College of Science, University of Sulaimani, Qlyasan Street, Sulaimani 46001, Kurdistan Region - F.R. Iraq

[5]Department of Medical Chemistry, College of Medicine, University of Duhok, Duhok, Kurdistan Region - F.R. Iraq

***Abstract*—In this work, the optical properties and optoelectronics parameters of binary and ternary composite films made of two electron acceptors, poly(L-Tryptophane) and poly(5-hydroxy-L-Tryptophane), with an electron donor, P(TER-CO-TRI), doped with Sudan dyes, are comprehensively investigated. The films with different volumetric ratios of the components were deposited onto the glass substrates using spin coating technique. Results showed that with the help of dye doping into the binary systems of poly(L-Tryptophane):P(TRI-co-TER) (1:2) and poly(5-hydroxy-L-Tryptophane):P(TRI-co-TER) (1:2), the refractive index was increased from 2.01 to 2.32. The nature of the electronic transition in the studied films was found to be a direct allowed transition, which was derived from Tauc's equation. The combination of cyclic voltammetry technique and absorption spectroscopy was used to determine the molecular energy levels, HOMO and LUMO of the polymer samples. It was seen that the mixture of poly(L-Tryptophane):P(TRI-co-TER):Sudan dye (1:2:2) has led to increase the energy gap to 2.95 eV and the real optical conductivity (σ_r) to about 433.11 S.cm^{-1}. According to the findings, the investigated polymers can have a great potential for semitransparent organic solar cells.**

ARO-The Scientific Journal of Koya University
Vol. XI, No. 1 (2023), Article ID: ARO.11103. 11 pages
Doi: 10.14500/aro.11103
Received: 31 October 2022; Accepted: 31 March 2023
Regular research paper: Published: 17 April 2023
Corresponding author's e-mail: fahmi.fariq@koyauniversity.org

***Index Terms*—Poly(L-Tryptophane), Poly(5-hydroxy-L-tryptophane), P(TER-CO-TRI), Sudan dye, Energy band gap, Refractive index, Dielectric constant.**

I. Introduction

Since the emergence of organic-material-based electronic devices, a variety of organic materials have been the subject of investigation. This can be mainly due to the distinctive properties of organic materials such as solution processability, thermal stability, lightweight, flexibility, high emission yield, and energy gap tuneability (Rajeswaran, et al., 2009; Sajid, et al., 2015; Lewis, 2006; Kaltenbrunner, et al., 2013). However, performance and operation of organic devices necessitate exhaustive studies of organic semiconductors (Gather, Köhnen and Meerholz, 2011). As a result, obtaining sufficient information on the optoelectronic properties of the used organic materials under various doping situations is essential to fabricate an efficient optoelectronic device. The process of doping can be used to fine-tune the optical characteristics of a material to the preferred level, in which the doped material acts as a host for the dopant material (Basir, et al., 2021). Herein, the aim is to take advantage of the dopant's significant features while concurrently improving the host response. Consequently, tris(8-hydroxyquinoline) aluminum (Alq_3) and its counterpart, tris (8-hydroxyquinolinate) Gallium Gaq3, were broadly employed in the electronic devices based on organic materials such as light-emitting diodes. They are preferred due to their superior thermal stability, optical

 http://dx.doi.org/10.14500/aro.11103

performance, and optoelectronic response. In addition, Alq3 has been successfully engaged in the fabrication of organic solar cells as an electron transport layer (El Jouad, et al., 2016; Muhammad and Sulaiman, 2018). As a result, Alq3 is a potential dopant for tuning the optoelectronic characteristics of organic semiconductors. In addition, N, N' -Di [(1-naphthyl)-N, N' - diphenyl]-(1, 1' -biphenyl)-4, 4' -diamine was used as a donor material in ultraviolet (UV) photodiodes (Vickers, 2017). One of the characteristic features of organic semiconductors is the tunability of electronic energy levels, which consequently leads to the energy gap tailoring of the active layers, thereby realizing photodetectors for simultaneous sensing of UV and infrared light (Muhammad, et al., 2017; Omidvar, 2017; Yang, et al., 2019). Moreover, it was seen from the literature that a hybrid composition of inorganic and organic materials can also be utilized to improve UV detectors (Hu, et al., 2015; Bilgaiyan, et al., 2017; Garg, et al., 2019). As a result, finding a potential candidate for an organic composite to be used as the active layer of UV detectors is critical. Many researchers have made significant efforts to utilize inorganic-based semiconductors or their hybrid nanoarchitectures and have primarily undertaken research employing these materials (Hou, et al., 2011; Jheng, et al., 2020). Applications such as imaging, medical sensing, secure communication, and assessment of many surrounding surroundings are conceivable thanks to UV ray detection, and active research is underway (Zeng, et al., 2019).

To address organic materials and their viability for potential applications, in this current work the absorption response, optical energy gap, refractive index, dielectric constant, and optical conductivity of organic composite systems incorporating poly(L-tryptophane) and poly(L-Tryptophane):P(TRI-co-TER) with Sudan dye are investigated.

II. Materials and Methods

Poly(5-hydroxy-L-Tryptophane) and poly(L-Tryptophane) are electron acceptors and P(TRI-co-TER) present an electron donor material. The molecular structures of the used materials are shown in Fig. 1. The organic materials were separately put inside vials and dissolved in chloroform solvent following their stirring overnight using a magnetic stirrer. Later on, the solutions of poly(5-hydroxy-L-Tryptophane), poly(L-Tryptophane), and P(TRI-co-TER) were prepared with concertation of 30 mg/mL. The composite binary films were made by volumetric compositions of Acceptor: Donor through mixing poly(5-hydroxy-L-Tryptophane), and poly (L-Tryptophane) with P(TRI-co-TER). Then, Sudan dye was also used to form a ternary composite system. The area under the absorption curve was calculated for all volume ratios of binary systems, and it was determined that (1:2) is the optimal volume ratio. As a result, the optoelectronic properties of the composite at this ratio were thoroughly examined. The optimized system was then doped by Sudan dye to produce a ternary system with different ratios of the dye as follows 1:2:1, 1:2:2 and 1:2:3. The thickness of the grown films was measured using Field emission scanning electron microscopy (FE-SEM) technique (TESCAN MIRA3 FEG-SEM) and the calculated values are shown in Table I. Furthermore, the structural investigation of the single, binary, and ternary films was carried out using the X-ray diffraction (XRD) spectra (Malvern Panalytical's X'Pert, using CuK alpha radiation [1.5418]).

III. Results and Discussion

A. Photophysical Properties

The optical properties of the polymers and their composite systems were assessed by UV-Vis absorption spectroscopy, as shown in Fig. 2. Despite the fact that intramolecular charge transfer (ICT) occurs at the main polymer chains between an electron deficient and an electron rich moiety due to visible absorption, it is also well known that the $\pi - \pi^*$ and $n - \pi^*$transitions of delocalized excitons occur in the polymer chain due to UV absorption. (Wang, et al., 2018; Shim, et al., 2015; Kim, et al., 2018). The absorption coefficient spectra of the polymers were determined using the following equation (Alsoghier, et al., 2018; Amin, et al., 2021):

$$\alpha = \frac{2.303A}{t} \quad \alpha = \frac{2.303A}{t} \tag{1}$$

Where t is the thickness of the film, and A is the absorbance of the studied sample. Noticeably, as shown in Fig. 2a and b, the two acceptor polymers exhibited a sharp absorption band in the UV region and extended to the visible region. The absorption band for the acceptor, poly(L-

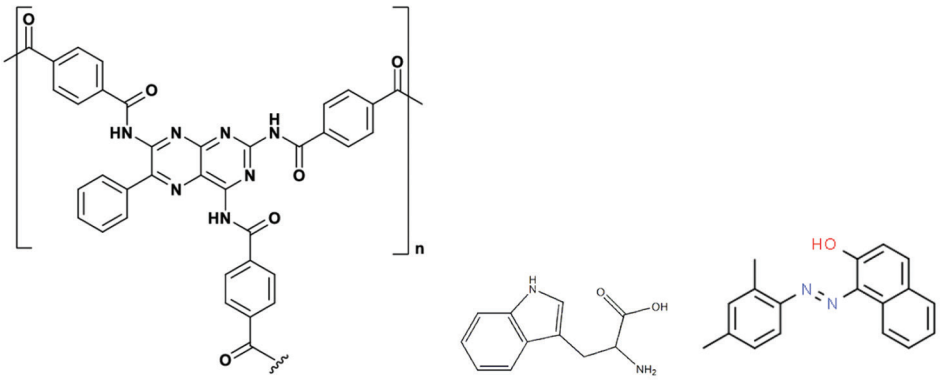

Fig. 1. Molecular structure of poly(triamterene-co-terephthalate), poly(L-tryptophan) and Sudan dye (left to right).

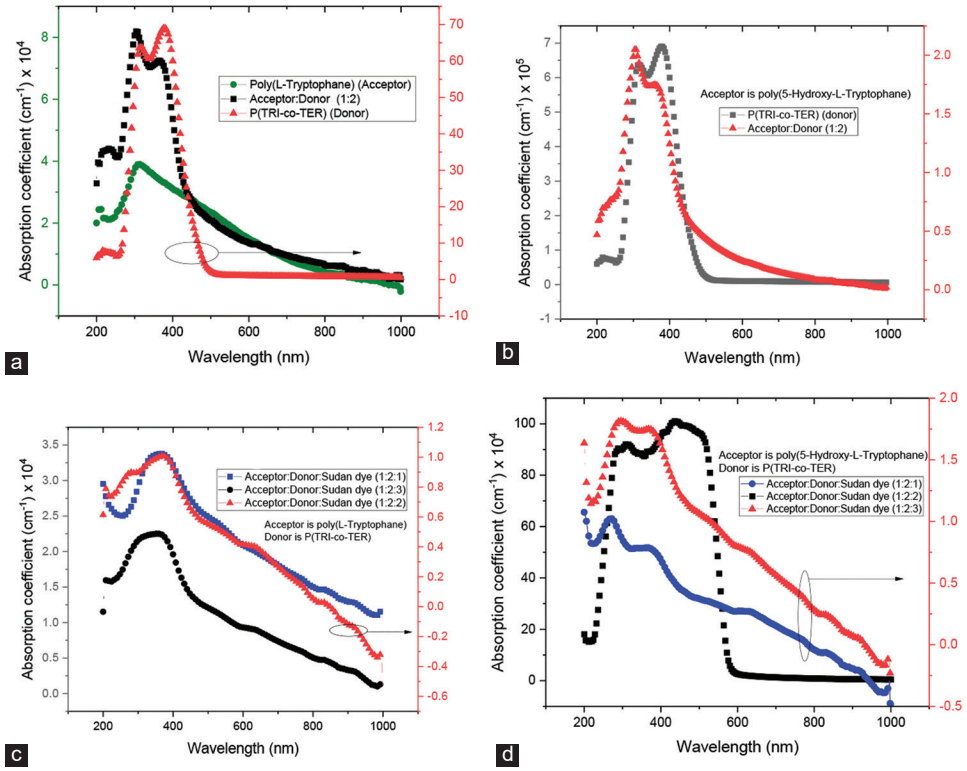

Fig. 2. Absorption coefficient spectra (a and b) of the studied polymers and binary films, and (c and d) ternary films.

TABLE I
THE MEASURED THICKNESS OF THE STUDIED ORGANIC FILMS

Film	Thickness (nm)
P (TRI-co-TER)	424
Poly (5-hydroxy-L-Tryptophane)	170
Poly (5-hydroxy-L-Tryptophane):P (TRI-co-TER) (1:2)	656
Poly (L-Tryptophane)	290
Poly (L-Tryptophane):P (TRI-co-TER) (1:2)	105
Poly (L-Tryptophane):P (TRI-co-TER):Sudan dye (1:2:1)	142
Poly (L-Tryptophane):P (TRI-co-TER):Sudan dye (1:2:2)	191
Poly (L-Tryptophane: P (TRI-co-TER):Sudan dye (1:2:3)	335
Poly (5-hydroxy-L-Tryptophane) :P (TRI-co-TER):Sudan dye (1:2:1)	275
Poly (5-hydroxy-L-Tryptophane) :P (TRI-co-TER):Sudan dye (1:2:2)	274
Poly (5-hydroxy-L-Tryptophane) :P (TRI-co-TER):Sudan dye (1:2:3)	227

Tryptophane) was prolonged to 424 nm, while that for poly(5-hydroxy-L-Tryptophane) was extended to 503 nm. The absorption band for the donor, P(TRI-co-TER) was continued till 468 nm, while the absorption band for the composite of poly(L-Tryptophane):P(TRI-co-TER) reached 474 nm. Noteworthy, on the addition of Sudan into the donor-acceptor system (Fig. 2c and d), the ternary composite structure has led to extending the absorption edge. This indicates that the strength of electronic transitions from π – π* has increased which is brought about by the addition of Sudan dye.

B. Optical Energy Gap and Transition Types

In optoelectronic applications, the measurements of the optical energy gap of the conjugated polymers and the type of electronic transitions are imperative. Hence, from the absorption spectra, it is plausible to measure the optical energy gap (Table II) and optical transition using Tauc's equation shown as Equation 3 (Muhammad and Sulaiman, 2011; Hamad, 2013). Alternately, the optical energy gap can be determined from the absorption spectrum by measuring the absorption edge of the spectrum, λ_{onset} as follows (Leonat, Sbârcea and Brañzoi, 2013):

$$E_g = \frac{1242}{\lambda_{onset}} \quad (2)$$

However, the nature of the transition can be assigned directly by Tauc's equations in addition to measuring the optical energy gap. Therefore, by taking the natural logarithm and derivation of Equation 3:

$$\alpha h\nu = \alpha_o (h\nu - Eg)^s \quad (3)$$

$$\frac{dln(\alpha h\nu)}{d(h\nu)} = \frac{s}{h\nu - Eg} \quad \frac{dln(\alpha h\nu)}{d(h\nu)} = \frac{s}{h\nu - Eg} \quad (4)$$

where α_o is an energy-independent constant, E_g is the energy gap, ν is the frequency of the incident wave, h is Planck's constant, and the value of s defines the type and nature of the transitions. If the value of s = 2, the transition is an indirectly allowed transition, s = 3 for indirectly forbidden transitions, s = 1/2 for directly allowed transitions and s = 3/2 for directly forbidden transitions. Fig. 3a depicts

http://dx.doi.org/10.14500/aro.11103

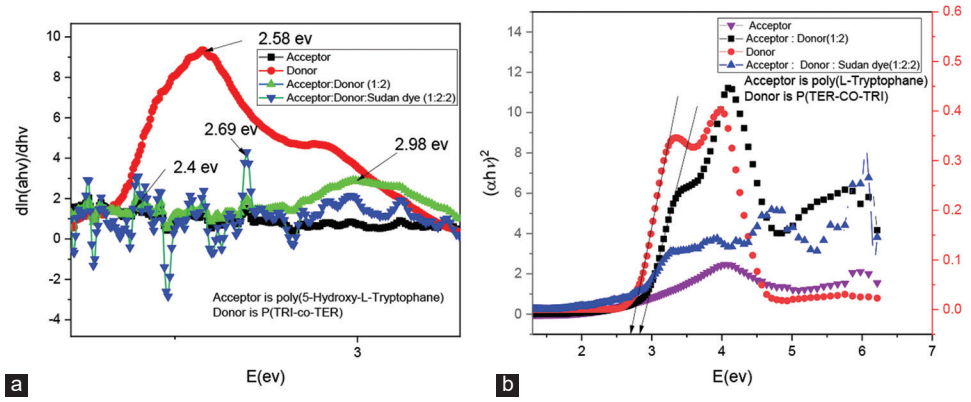

Fig. 3. Plot of $\frac{dln(\alpha hv)}{d(hv)}$ versus hv (a), and $(\alpha hv)^2$ versus E (b) for the representative films.

TABLE II
DETERMINED ENERGY GAP FOR THIN FILM OF THE POLYMERS AND TERNARY COMPOSITES

Materials	E_g^{Tauc} (eV)
P (TRI-co-TER)	2.66
Poly (L-Tryptophane)	2.61
Poly (L-Tryptophane):P (TRI-co-TER) (1:2)	2.85
Poly (L-Tryptophane):P (TRI-co-TER):Sudan dye (1:2:2)	2.95
Poly (5-hydroxy-L-Tryptophane)	2.34
Poly (5-hydroxy-L-Tryptophane):P (TRI-co-TER) (1:2)	2.89
Poly (5-hydroxy-L-Tryptophane): P (TRI-co-TER):Sudan dye (1:2:2)	2.60

the plots of $\frac{dln(\alpha hv)}{d(hv)}$ versus hv for all the samples and from which the approximate value of energy gap, $hv = E_g$ was taken at the peak value. Hereafter, the estimated value of E_g was employed for plotting $ln(\alpha hv)$ versus $ln(hv - Eg)$ and from the slope of the curves the value of s was determined and it was found to be $\frac{1}{2}$, which is the evidence of the occurrence of a direct allowed transition between the intermolecular energy bands of the polymers. Henceforward, the accurate values of the energy gaps were determined by plotting $(\alpha hv)^2$ as a function of (hv) and taking the extrapolation of the linear portion at $(\alpha hv)^2 = 0$, as shown in Fig. 3b.

C. Electrochemical Properties

In designing and optimizing electronic devices based organic materials, several parameters should be revealed that define the nature of charge transfer and charge collection. To this end, the position of electronic energy levels (HOMO and LUMO) of organic semiconductor materials can be determined by electrochemical study before device fabrication. Therefore, cyclic voltammetry (CV) is a worthy technique to estimate energy levels for the relevant materials from the oxidation and reduction potentials. Hence, the oxidation and reduction potentials are infer from the onset potential, which is defined as the potential, where electrons or holes are initially injected into the LUMO and HOMO levels, respectively, and the rise of anodic or cathodic current becomes obvious (Johansson, et al., 2003). Thus, the position of the HOMO and LUMO levels was first estimated by measuring the optical energy gaps from Tauc's equation, as was discussed previously. Then, from the equations below, the HOMO and LUMO levels were estimated using ferrocene as the reference couple (Cardona, et al., 2011) (Alqurashy, et al., 2020):

$$E_{HOMO} = -)E(_{onset,oxvs.Fc+/Fc}) + 5.39)\ (eV) \quad (5)$$

$$E_{LUMO} = -(E(_{onset,redvs.Fc+/Fc}) + 5.39)\ (eV) \quad (6)$$

$$E_g^{Tauc} = E_{HOMO} - E_{LUMO} \quad (7)$$

Where $E(_{onset,oxvs.Fc+/Fc})$ and $E(_{onset,redvs.Fc+/Fc})$ represent the onset potential of the oxidation and reduction potential, respectively. The value of 5.39 represents the formal potential of the Fc^+/Fc redox couple versus vacuum. Fig. 4 shows the CV spectra of the polymers versus Fc/Fc+, while their corresponding electrochemical parameters are shown in Table III. The HOMO level is influenced by the type of substituents (whether electron withdrawing or electron donating species) and it can be seen that P(TRI-co-TER) experienced a high HOMO level compared to poly(L-Tryptophane) polymer. This could be due to the presence of the indole N–H group (Huang, et al., 2015). In addition, the LUMO level of P(TRI-co-TER) is 2.78 eV but LUMO levels of the acceptors, namely, poly(L-Tryptophane) and poly(5-hydroxy-L-Tryptophane), are 2.87 eV and 3.19 eV, respectively.

D. Optical Constants

Optical constants reveal the nature of interactions between organic materials and the electromagnetic spectrum. For instance, the loss of the incident photon due to scattering and absorption within the film is ascribed by the extinction coefficient (k). In addition, another constant entitled the optical dielectric constant (ε), which is a frequency dependent parameter, demonstrates the electronic response of the material when interacts with photons. Meanwhile, the dielectric constant is a complex function and its real part is assigned to polarization on the impact of an electromagnetic

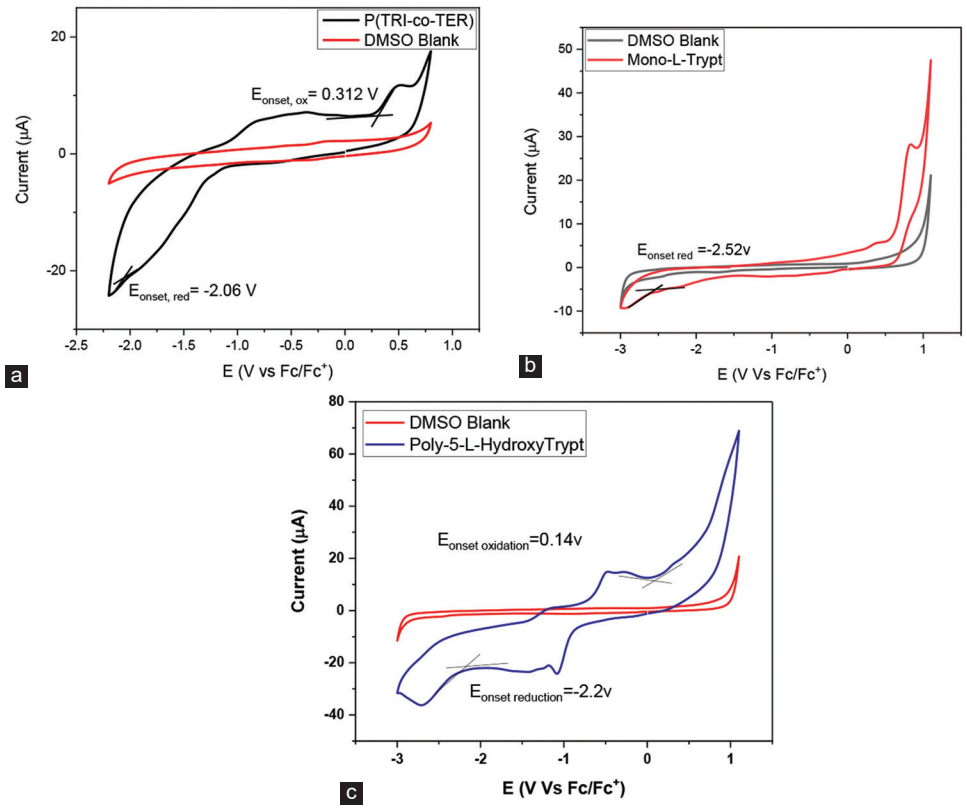

Fig. 4. The cyclic voltammetry of (a) P(TRI-co-TER), (b) poly(L-Tryptophane), and (c) poly(5-hydroxy-L-Tryptophane).

TABLE III
ELECTROCHEMICAL AND OPTICAL DATA FOR ALL SYNTHESIZED POLYMERS

Polymer	$E_{onset,ox}$ (V)	$E_{onset,red}$ (V)	E_{HOMO} (eV)	E_{LUMO} (eV)	E_g (eV)
P (TRI-co-TER)	0.312	-1.24	-5.70	-2.78	2.92
Poly(L-Tryptophane)	NA	-2.52	-5.39	-2.87	2.52
Poly (5-hydroxy-L-Tryptophane)	0.14	-2.20	-5.53	-3.19	2.34

field, while the imaginary part illustrates the optical loss. The following equations were sequentially used to calculate the optical parameters of the studies films (Fariq, Shujahadeen, and Hussein, 2015).

$$n = \frac{-2(R+1) - \sqrt{4k^2R^2 + 16R - 4k^2}}{2(R-1)} \quad (8)$$

$$k = \frac{\alpha\lambda}{4\pi} \quad (9)$$

$$\varepsilon = \varepsilon_r + i\varepsilon_i \quad (10)$$

$$\varepsilon_r = n^2 - k^2 \quad (11)$$

$$\varepsilon_i = 2nk \quad (12)$$

$$Tan\delta = \varepsilon_i / \varepsilon_r \quad (13)$$

Where ε_r represents the real part, ε_i is the imaginary part of the dielectric constant, n is the refractive index, k is the extinction coefficient, and R is the reflectance. Figs. 5 and 6 shows the real and imaginary dielectric constant spectra of the investigated films, while Fig. 7a and b shows the extinction coefficient in the wavelength range from 200 to 1000 nm for composite systems. Noticeably, it can be seen that the real part of the optical dielectric constant spectrum reflects the spectrum of refractive index (Fig. 8) because of the small value of k, while the spectrum of the imaginary part is essentially related to the spectrum of the absorption coefficient (see Eqs. 9, 11 and 12). Table IV shows that the real dielectric constant for the poly(L-Tryptophane), poly(5-hydroxy-L-Tryptophane), and P(TRI-co-TER) is lower than those of their mixed structures in the binary and ternary forms (Rahim, et al., 2022)

Fig. 8a and b shows the refractive index of the studied thin film in the wavelength range from 200 to 1000 nm. Therefore, it was perceived that refractive index follows an inconsistent dispersion in both UV and near visible region, while a non-dispersive response observed in the IR region (transparent region). In addition, the infinite refractive index (n_∞) can be experimentally extracted from the non-dispersive/flattened portion of the refractive index spectrum and its values for the investigated films were shown in Table IV. Hence, the refractive index values are shown in Table IV, which were obtained from the plateau region of the spectra shown in Fig. 8a and b. It was observed form Fig. 8a that the P(TRI-co-TER) (n = 1.82) and poly(L-Tryptophane) (n = 1.62) are lower than that of the mixed A: D (1:2) (n = 2.01) and A: D:Sudan dye (1:2:2) (n = 2.32). Interestingly, with the help of poly(L-Tryptophane) (n = 1.62) dopant, it is possible to increase the refractive index of P(TRI-co-TER) from 1.82 to 2.01 and to 2.32 in the binary and ternary systems, respectively. Similarly, as shown in Fig. 8b, with the help

http://dx.doi.org/10.14500/aro.11103

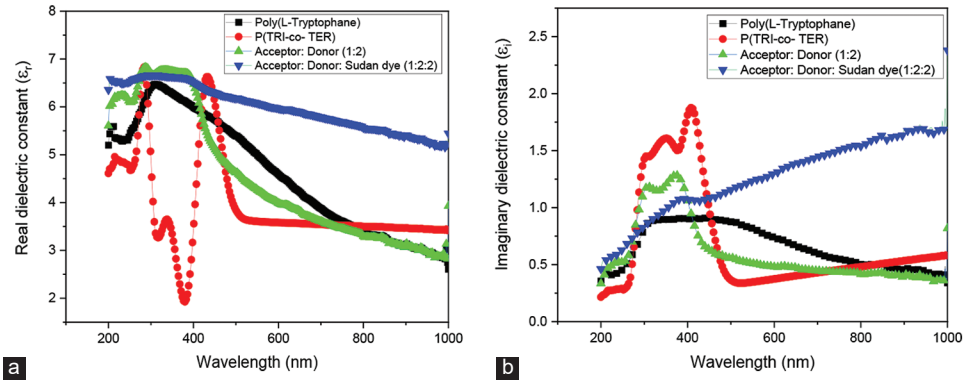

Fig. 5. Dielectric constant spectra, (a) real part and (b) imaginary part, for the poly(L-Tryptophane), P(TRI-co-TER), their binary and ternary systems.

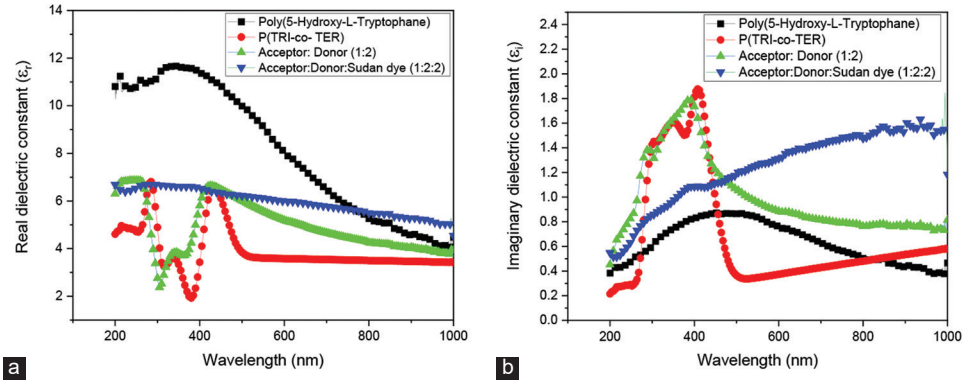

Fig. 6. Dielectric constant spectra, (a) real part and (b) imaginary part, for poly(5-hydroxy-L-Tryptophane), P(TRI-co-TER), their binary and ternary systems.

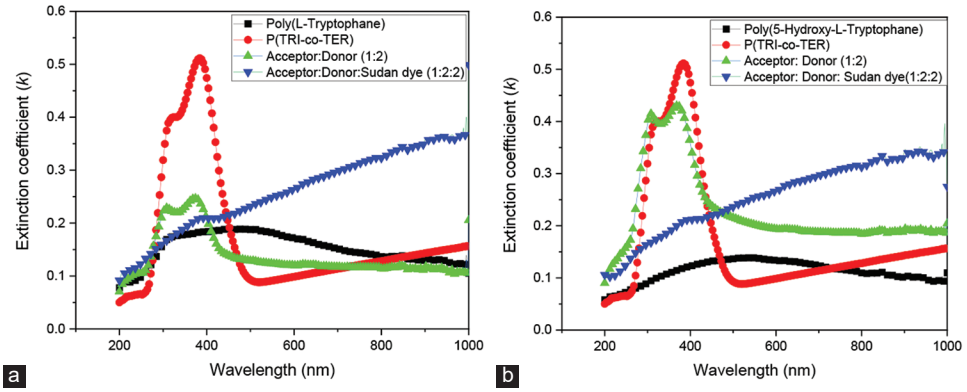

Fig. 7. Extinction coefficient spectra of poly(L-Tryptophane), poly(5-hydroxy-L-Tryptophane), P(TRI-co-TER), their binary and ternary systems.

TABLE IV
THE OPTOELECTRONIC PARAMETERS OF THE INVESTIGATED THIN FILMS

Materials	n	ε_r	σ_r (S.cm^{-1})
P (TRI-co-TER)	1.82	3.29	89.67
Poly (L-Tryptophane)	1.62	2.61	56.86
Acceptor: Donor (1:2)	2.01	3.99	145.19
Acceptor: Donor: Sudan dye (1:2:2)	2.32	5.02	433.11
Poly (5-hydroxy-L-Tryptophane)	1.79	3.19	36.09
Acceptor: Donor (1:2)	1.98	3.85	132.91
Acceptor: Donor: Sudan dye (1:2:2)	2.32	4.98	439.07

of dopant poly(5-hydroxy-L-Tryptophane) (n = 1.79), the refractive index was increased to 1.98 and 2.32, the binary and ternary systems, respectively. This trend was found to be consistent with those described in the literature (Holzer, Penzkofer, and Hörhold, 2000). Consequently, it was found that the refractive index and real optical conductivity (Fig. 9) are increased with the addition of the second and third dopant components into the polymers. This can be ascribed to the increased conjugation bonds and better packing compact between the molecular arrangements of the structures, thereby reducing the speed of the incident light waves by a larger degree.

Furthermore, Figs. 9 and 10 exhibit the spectra of the optical conductivity of both composite systems and the real and imaginary components of optical conductivity

$(\sigma^* = \sigma_r + i\sigma)\sigma^* = \sigma_r + i\sigma_i$ can be investigated by means of the following formulas:

$$\sigma_r = \omega\varepsilon_o\varepsilon_i \quad \sigma_r = \omega\varepsilon_o\varepsilon_i \tag{14}$$

$$\sigma_i = \omega\varepsilon_o\varepsilon_r \quad \sigma_i = \omega\varepsilon_o\varepsilon_r \tag{15}$$

Where σ_r is the real optical conductivity, σ_i is the imaginary optical conductivity, ω is the angular frequency, and ε_o is free space permittivity ($8.85\times10^{-12} F/m$). Figs. 9a and 10 reveal that, at long wavelengths, the values of real optical conductivity for both composite systems remain constant (non-dispersive). Figs. 9a and 10a reveal that, at long wavelengths, the values of real optical conductivity for both composite systems remain constant (non-dispersive). This indicates that the change in optical conductivity is directly related to the variation of excited electrons due to the absorption of photon energy by the thin film.

Therefore, the increment in the optical absorption of the obtained samples in the UV region is a consequence of increased optical conductivity and vice versa. Figs. 9b and 10b shows the imaginary optical conductivity for poly (L-Tryptophane), poly (5-hydroxy-L-Tryptophane), P (TRI-co-TER), along with the binary and ternary systems. In addition, the dissipation factor (DF) is a measure of loss-rate of energy of a mode of oscillation (mechanical, electrical, or electromechanical) in a dissipative system. It is the reciprocal of quality factor, which represents the "quality" or durability of oscillation. It was seen from Fig. 11a and b that the DF for the donor system is larger than that of the other samples. Furthermore, a comparison between the major optoelectronic parameters of some polymers from literature and those achieved in the current study was carried out, as shown in Table V.

E. Morphological Properties

FE-SEM is a widely used technique to investigate the surface morphology, microstructure, grain size, and shape of the films. Fig. 12 depicts the FE-SEM images of the films, in which the shape of grains is found to be of different sizes and randomly distributed along the substrate surface. The average particle size on the surface of the acceptors and donor films was increased significantly compared to the binary and ternary films. It was seen that the number of pores increased when dopant concentration was increased (Trinh, et al., 2011).

F. Structural Properties

The X-ray diffraction patterns were used to characterize the structure of the studied films deposited on the glass substrate. Poly(L-Tryptophane) and poly(5-hydroxy-L-Tryptophane) acceptors and P(TER-CO-TRI) donor mixed with Sudan dye thin films were coated on the glass substrates and their XRD patterns were recorded in the

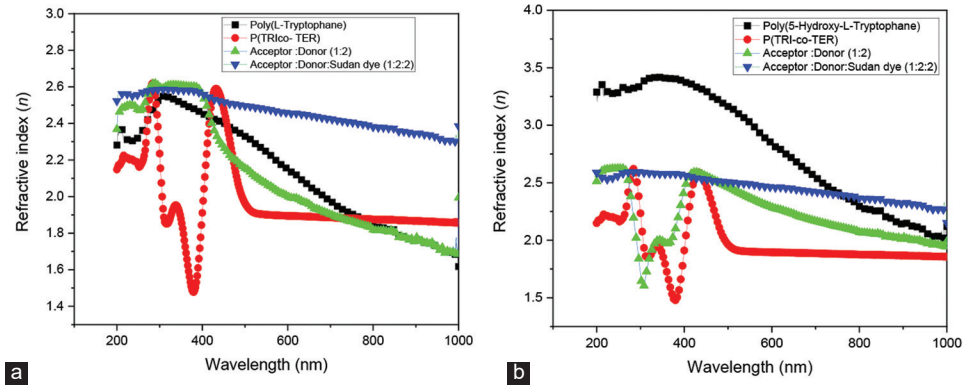

Fig. 8. (a and b) Refractive index spectra of poly(L-Tryptophane), poly(5-hydroxy-L-Tryptophane), P(TRI-co-TER), their binary and ternary systems.

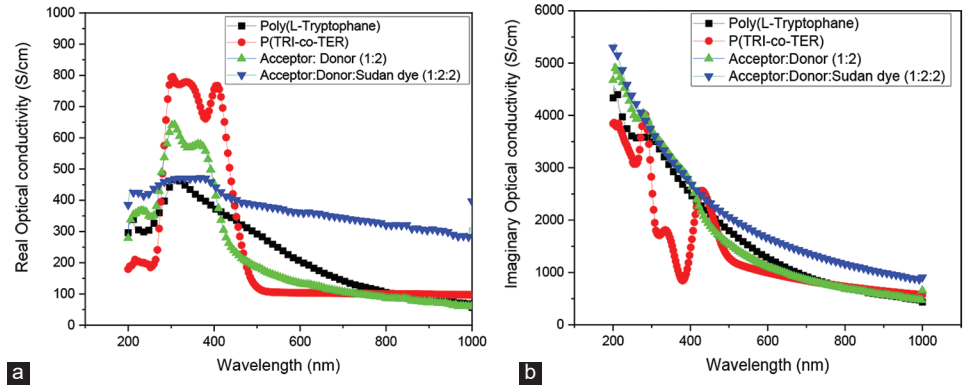

Fig. 9. Optical conductivity spectra of poly(L-Tryptophane) and its composite systems; (a) real part and (b) imaginary part.

http://dx.doi.org/10.14500/aro.11103

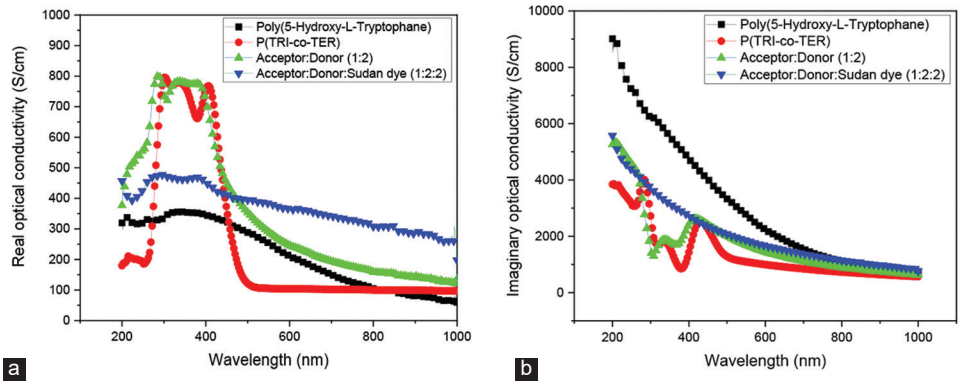

Fig. 10. Optical conductivity spectra of poly(5-hydroxy-L-Tryptophane) and its composite systems; (a) real part and (b) imaginary part.

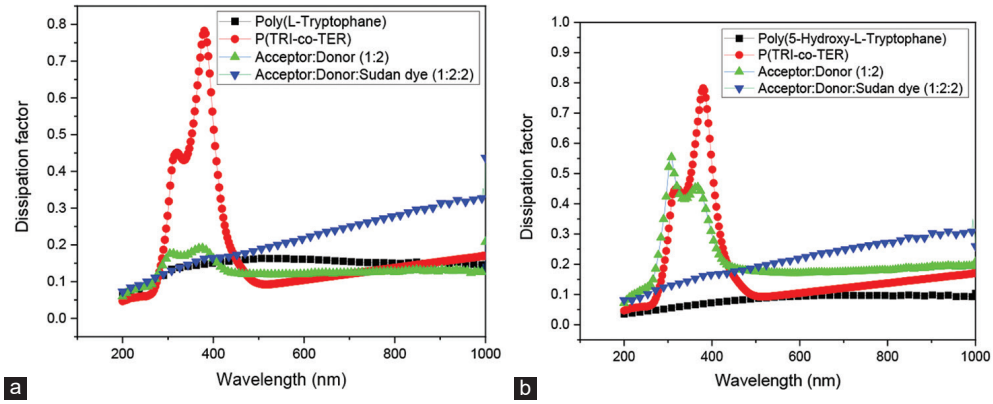

Fig. 11. Dielectric lost tangent (dissipation factor) spectra of poly(L-Tryptophane), poly(5-hydroxy-L-Tryptophane), P(TRI-co-TER), their binary and ternary systems.

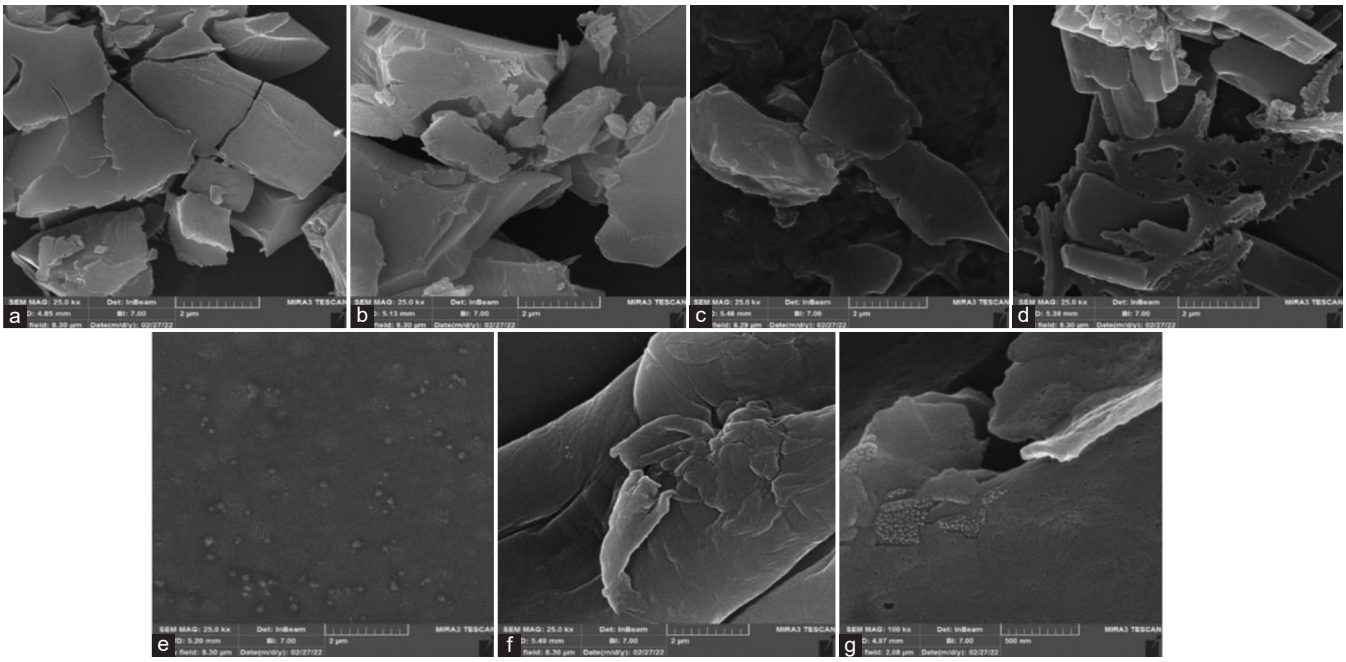

Fig. 12. The field emission-scanning electron microscopy image of (a) P(TER-co-TRI), (b) Poly(L-Tryptophane), (c) poly(L-Tryptophane):P(TER-CO-TRI) (1:2), (d) Poly(L-Tryptophane):P(TER-co-TRI):Sudan dye (1:2:2), (e) Poly(5-hydroxy-L-Tryptophane), (f) Poly(5-hydroxy-L-Tryptophane):P(TER-co-TRI) (1:2) and (g) Poly(5-hydroxy-L-Tryptophane):P(TER-co-TRI):Sudan dye (1:2:2).

TABLE V
COMPARISON BETWEEN SOME POLYMERS AND THE INVESTIGATED THIN FILMS IN TERMS OF THE MAIN OPTOELECTRONIC PARAMETERS.

Materials	E_g (eV)	n	ε_r	References
P (TRI-co-TER)	2.92	1.82	3.29	This work
Poly(L-Tryptophane)	2.52	1.62	2.61	This work
Poly (5-hydroxy-L-Tryptophane)	2.34	1.79	3.19	This work
Polyvinylpyrrolidone (PVP)	2.40	1.49	3.60	Shubha, Manohara and Gerward, 2017
PHPMIVP	1.85	1.60	3.80	Barrillon, et al., 2023
Poly (ethylene oxide) PEO	2.60	1.45	2.20	Abd El-Kader and Elabbasy, 2020
Polyisoprene	1.04	1.52	2.50	Fan, et al., 2020

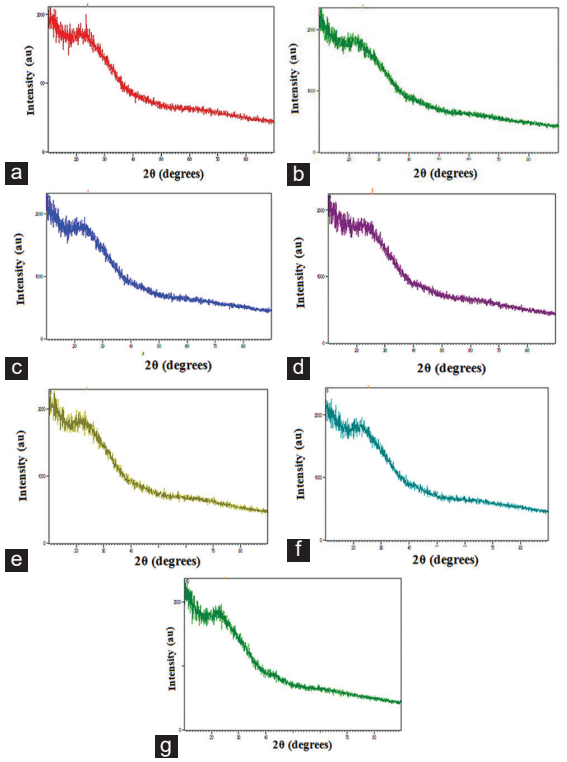

Fig. 13. The X-ray diffraction pattern of (a) P(TER-co-TRI), (b) Poly(L-Tryptophane), (c) poly(L-Tryptophane):P(TER-CO-TRI) (1:2), (d) Poly(L-Tryptophane):P(TER-co-TRI):Sudan dye (1:2:2), (e) Poly(5-hydroxy-L-Tryptophane), (f) Poly(5-hydroxy-L- Tryptophane):P(TER-co-TRI) (1:2) and (g) Poly(5-hydroxy-L-Tryptophane):P(TER-co-TRI):Sudan dye (1:2:2).

range of 2θ between 10° and 90°. Fig. 13 shows the XRD diffraction patterns of the films. The poly(L-Tryptophane) and poly(5-hydroxy-L-Tryptophane) along with the binary and ternary films they all showed abroad bump in the low angle of diffraction, which indicates their amorphous nature. However, the dopant P(TER-CO-TRI) films showed a single sharp diffraction peaks at 24o, which corresponds to a d-spacing of 3.72 Å. Furthermore, its low intensity could be used as indicator for the small particle size (Al-Dulaimi, et al., 2017). Therefore, this peak indicates the intermolecular distance between two neighboring planes, which is obtained by Bragg's equation:

$$n \lambda = 2d \sin\theta \quad (16)$$

Where n (an integer) is the "order" of reflection, λ is the wavelength of the incident X-rays, d is the interplanar spacing of the crystal and θ is the angle of incidence (Kato, Ito and Hoshino, 2020).

G. Photoluminescence (PL) Properties

To investigate the PL spectrum of the films, they were excited by 355 nm exciting laser. the PL spectra of Poly(L-Tryptophane),Poly(5-hydroxy-L- Tryptophane), binary and ternary films are illustrated in Fig. 14a and b. All films showed a typical UV emission peak centered at about 350 nm, near the band edge of binary and ternary. The charge transfer behavior of the acceptor and donor (A/D) between layer and acceptors layer is examined by the PL spectroscopy measurements. One can notice from Fig. 14a and b that the peak position of the emission is red shifted for the binary system compared to that of the single film. Furthermore, the peak position for the ternary film is red shifted compared to that of the binary film. This red shifting is a clear evidence of the change in the electronic distribution of the system with the addition of the second and third components, implying the change in the energy band gaps, as was explained in the previous sections. Another feature of the PL peak is that its intensity has decreased in the ternary films compared to that of the binary ones. This indicates the more efficient charge transfer between the moieties of the acceptor and donor components on the absorption of light by the electronic states.

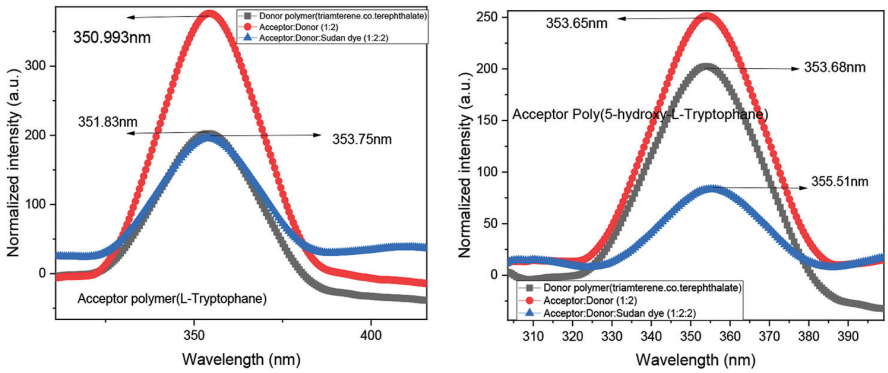

Fig. 14: Photoluminescence spectra of the investigated films in binary and ternary composite forms.

IV. Conclusions

In this work, a broad investigation on the optical properties and optoelectronic parameters of P(TER-CO-TRI), poly(L-Tryptophane), and poly(5-hydroxy-L-Tryptophane) along with their doping with Sudan dye was successfully performed. Optical spectroscopy was seen to be highly effective to measure the optoelectronic parameters of the binary and ternary composites made from the polymer materials and the dye. It was concluded that with the help of doping process, different values of energy band gap, refractive index, dielectric constant, and optical conductivity are achieved. This tuning achievement of the optoelectronic parameters plays a key role in shaping the possible applications of these materials in organic electronics, photodiodes, and photovoltaic devices. The nature of the electronic transition in the studied samples was confirmed to be a direct allowed transition, which was derived from the application of Tauc's equation. The combination of CV test and absorption spectroscopy was successfully used to determine the molecular energy levels, HOMO, and LUMO of the polymer samples.

V. Acknowledgment

Kamal A. Ketuly thanks the Erasmus + scheme for facilitating collaboration between the University of Duhok and the University of Glasgow.

VI. Conflicts of Interest

The authors declare that there are no conflicts of interest regarding the publication of this paper.

VII. Authors' Contributions

Methodology: Barham Kamal Rahim; Conceptualization: Fahmi F. Muhammadsharif and Salah Raza Saeed; Writing - original draft preparation: Barham Kamal Rahim; Writing-review and editing: Fahmi F. Muhammadsharif, Salah Raza Saeed, Kamal Aziz Ketuly; Formal analysis and investigation: Fahmi F. Muhammadsharif, Salah Raza Saeed, Kamal Aziz Ketuly; Supervision: Fahmi F. Muhammadsharif, Salah Raza Saeed.

VIII. Availability of Data and Materials

The data and material are available within the manuscript.

References

Abd El-Kader, M.F.H. and Elabbasy, M.T. (2020). Gamma radiation modified the optical, electrical, and antibacterial characterization of CuONPs doped in polyethylene oxide/polyvinyl alcohol. *Journal of Materials Research and Technology*, 9(6), pp. 16179-16185.

Al-Dulaimi, N., Lewis, E.A., Savjani, N., McNaughter, P.D., Haigh, S.J., Malik, M.A., Lewis, D.J. and O'Brien, P. (2017). The influence of precursor on rhenium incorporation into Re-doped MoS2 (Mo1-:XRexS2) thin films by aerosol-assisted chemical vapour deposition (AACVD). *Journal of Materials Chemistry C*, 5(35), pp. 9044-9052.

Alqurashy, B.A., Iraqi, A., Zhang, Y. and Lidzey, D.G. (2020). Pyrene-benzo[1,2,5]thiadiazole based conjugated polymers for application in BHJ solar cells. *Journal of Saudi Chemical Society*, 24(6), pp. 484-491.

Alsoghier, H.M., Selim, M.A., Salman, H.M.A., Rageh, H.M., Santos, M.A., Ibrahim, S.A., Dongol, M., Soga, T. and Abuelwafa, A.A. (2018). NMR spectroscopic, linear and non-linear optical properties of 1,3-benzothiazol-2-yl-(phenylhydrazono)acetonitrile (BTPA) azo dye. *Journal of Molecular Structure*, 1179, pp. 315-324.

Amin, P.O., Ketuly, K.A., Saeed, S.R., Muhammadsharif, F.F., Symes, M.D., Paul, A. and Sulaiman, K. (2021). Synthesis, spectroscopic, electrochemical and photophysical properties of high band gap polymers for potential applications in semi-transparent solar cells. *BMC Chemistry*, 15(1), p. 25.

Barrillon, S., Fuchs, R., Petrenko, A.A., Comby, C., Bosse, A., Yohia, C., Fuda, J.L., Bhairy, N., Cyr, F., Doglioli, A.M., Grégori, G., Tzortzis, R., d'Ovidio, F. and Thyssen, M. (2023). Phytoplankton reaction to an intense storm in the north-western Mediterranean Sea. *Biogeosciences*, 20(1), pp. 141-161.

Basir, A., Alzahrani, H., Sulaiman, K., Muhammadsharif, F.F., Mahmoud, A.Y., Bahabry, R.R., Alsoufi, M.S., Bawazeer, T.M. and Ab Sani, S.F. (2021). An investigation on the optical parameters of TPD: Alq3 composite thin films. *Physica B: Condensed Matter*, 606, p. 412816.

Bilgaiyan, A., Dixit, T., Palani, I.A. and Singh, V. (2017). Performance improvement of ZnO/P3HT hybrid UV photo-detector by interfacial Au nanolayer. *Physica E: Low-Dimensional Systems and Nanostructures*, 86, pp. 136-141.

Cardona, C.M., Li, W., Kaifer, A.E., Stockdale, D. and Bazan, G.C. (2011). Electrochemical considerations for determining absolute frontier orbital energy levels of conjugated polymers for solar cell applications. *Advanced Materials*, 23(20), pp. 2367-2371.

Davis, E.A., Mott, N.F. (1970) Conduction in non-crystalline systems V. Conductivity, optical absorption and photoconductivity in amorphous semiconductors, *The Philosophical Magazine: A Journal of Theoretical Experimental and Applied Physics*, 22:179, 0903-0922, DOI: 10.1080/14786437008221061.

El Jouad, Z., Barkat, L., Stephant, N., Cattin, L., Hamzaoui, N., Khelil, A., Ghamnia, M., Addou, M., Morsli, M., Béchu, S., Cabanetos, C., Richard-Plouet, M., Blanchard, P. and Bernède, J.C. (2016). Ca/Alq3 hybrid cathode buffer layer for the optimization of organic solar cells based on a planar heterojunction. *Journal of Physics and Chemistry of Solids*, 98, pp. 128-135.

Fan, X., Xu, H., Wu, C., Song, Y. and Zheng, Q. (2020). Influences of chemical crosslinking, physical associating, and filler filling on nonlinear rheological responses of polyisoprene. *Journal of Rheology*, 64(4), pp. 775-784.

Fariq, F., Shujahadeen, M. and Hussein, S.A. (2015). Effect of the dopant salt on the optical parameters of PVA : NaNO 3 solid polymer electrolyte. 26, pp. 521-529.

Garg, M., Tak, B.R., Rao, V.R. and Singh, R. (2019). Giant UV photoresponse of GaN-based photodetectors by surface modification using phenol-functionalized porphyrin organic molecules. *ACS Applied Materials and Interfaces*, 11(12), pp. 12017-12026.

Gather, M.C., Köhnen, A. and Meerholz, K. (2011). White organic light-emitting diodes. *Advanced Materials*, 23(2), pp. 233-248.

Hamad, T.K. (2013). Refractive index dispersion and analysis of the optical parameters of (PMMA/PVA) thin film. *Journal of Al-Nahrain University Science*, 16(3), pp. 164-170.

Holzer, W., Penzkofer, A. and Hörhold, H.H. (2000). Travelling-wave lasing of TPD solutions and neat films. *Synthetic Metals*, 113(3), pp. 281-287.

Hou, Y.N., Mei, Z.X., Liang, H.L., Ye, D., Liang, S., Gu, C. and Du, X.L. (2011). Comparative study of n-MgZnO/p-Si ultraviolet-B photodetector performance with different device structures. *Applied Physics Letters*, 98(26), p. 263501.

Hu, Z.F., Huai-Hao, W., Yan-Wu, L. and Xi-Qing, Z. (2015). High response Schottky ultraviolet photodetector formed by PEDOT: PSS transparent electrode contacts to Mg0.1Zn0.9O. *Chinese Physics B*, 24(10), 107302.

Huang, Y., Wu, F., Zhang, M., Mei, S., Shen, P. and Tan, S. (2015). Synthesis and photovoltaic properties of conjugated polymers with an asymmetric 4-(2-ethylhexyloxy)-8-(2-ethylhexylthio)benzo[1,2-b:4,5-b′]dithiophene unit. *Dyes and Pigments*, 115, pp. 58-66.

Jheng, J.S., Wang, C.K., Chiou, Y.Z., Chang, S.P. and Chang, S.J. (2020). Voltage-tunable uvc-uvb dual-band metal-semiconductor-metal photodetector based on ga2o3/mgzno heterostructure by rf sputtering. *Coatings*, 10(10), p. 994.

Johansson, T., Mammo, W., Svensson, M., Anderssonb, M.R. and Inganäsa, O. (2003). Electrochemical bandgaps of substituted polythiophenes. *Journal of Materials Chemistry*, 13, pp. 1316-1323.

Kaltenbrunner, M., Sekitani, T., Reeder, J., Yokota, T., Kuribara, K., Tokuhara, T., Drack, M., Schwödiauer, R., Graz, I., Bauer-Gogonea, S., Bauer, S. and Someya, T. (2013). An ultra-lightweight design for imperceptible plastic electronics. *Nature*, 499(7459), pp. 458-463.

Kato, K., Ito, K. and Hoshino, T. (2020). Anisotropic amorphous X-ray diffraction attributed to the orientation of cyclodextrin. *Journal of Physical Chemistry Letters*, 11(15), pp. 6201-6205.

Kim, J., Chae, S., Yi, A., Hong, S., Kim, H.J. and Suh, H. (2018). Characterization of push-pull type of conjugated polymers containing 8H-thieno[2,3-b]indole for organic photovoltaics. *Synthetic Metals*, 245, pp. 267-275.

Leonat, L., Sbârcea, G. and Braȋnzoi, I.V. (2013). Cyclic voltammetry for energy levels estimation of organic materials. *UPB Scientific Bulletin, Series B: Chemistry and Materials Science*, 75(3), pp. 111-118.

Lewis, J. (2006). Material challenge for flexible organic devices. *Materials Today*, 9(4), pp. 38-45.

Muhammad, F.F. and Sulaiman, K. (2011). Utilizing a simple and reliable method to investigate the optical functions of small molecular organic films-Alq3 and Gaq3 as examples. *Measurement: Journal of the International Measurement Confederation*, 44(8), pp. 1468-1474.

Muhammad, F.F. and Sulaiman, K. (2018). Thermal stability and reproducibility enhancement of organic solar cells by tris(hydroxyquinoline)gallium dopant forming a dual acceptor active layer. *Aro-the Scientific Journal of Koya University*, 6(2), p. 69.

Muhammad, F.F., Yahya, M.Y., Aziz, F., Rasheed, M. and Sulaiman, K. (2017). Tuning the extinction coefficient, refractive index, dielectric constant and optical conductivity of Gaq3 films for the application of OLED displays technology. *Journal of Materials Science: Materials in Electronics*, 28(19), pp. 14777-14786.

Omidvar, A. (2017). Electronic structure tuning and band gap opening of nitrogen and boron doped holey graphene flake: The role of single/dual doping. *Materials Chemistry and Physics*, 202, 1-384.

Rahim, B.K., Muhammadsharif, F.F., Saeed, S.R. and Ketuly, K.A. (2022). A study on the optical properties and optoelectronic parameters of Sudan dye doped poly (5-hydroxy-L-tryptophane) and P (TER-CO-TRI) polymers. *Modern Electronic Materials*, 8(3), pp. 85-96.

Rajeswaran, M., Blanton, T.N., Tang, C.W., Lenhart, W.C., Switalski, S.C., Giesen, D.J., Antalek, B.J., Pawlik, T.D., Kondakov, D.Y., Zumbulyadis, N. and Young, R.H. (2009). Structural, thermal, and spectral characterization of the different crystalline forms of Alq3, tris(quinolin-8-olato)aluminum(III), an electroluminescent material in OLED technology. *Polyhedron*, 28(4), pp. 835-843.

Sajid, M., Zubair, M., Doh, Y.H., Na, K.H. and Choi, K.H. (2015). Flexible large area organic light emitting diode fabricated by electrohydrodynamics atomization technique. *Journal of Materials Science: Materials in Electronics*, 26(9), pp. 7192-7199.

Shim, J.Y., Kim, T., Kim, J., Kim, J., Kim, I., Kim, J.Y. and Suh, H. (2015). Trifluoromethyl benzimidazole-based conjugated polymers with deep HOMO levels for organic photovoltaics. *Synthetic Metals*, 205, pp. 112-120.

Shubha, A., Manohara, S.R. and Gerward, L. (2017). Influence of polyvinylpyrrolidone on optical, electrical, and dielectric properties of poly(2-ethyl-2-oxazoline)-polyvinylpyrrolidone blends. *Journal of Molecular Liquids*, 247, pp. 328-336.

Trinh, T.T., Tu, H.N., Huy, H.L., Ryu, K.Y., Le, K.B., Pillai, K. and Yi, J. (2011). Improving the ethanol sensing of ZnO nano-particle thin films-the correlation between the grain size and the sensing mechanism. *Sensors and Actuators, B: Chemical*, 152(1), pp. 73-81.

Vickers, N.J. (2017). Animal communication: When i'm calling you, will you answer too?. *Current Biology*, 27(14), pp. R713-R715.

Wang, J., Yin, P., Wu, Y., Liu, G., Cui, C. and Shen, P. (2018). Synthesis and optoelectronic property manipulation of conjugated polymer photovoltaic materials based on benzo[d]-dithieno[3,2-b;2′,3′-f]azepine. *Polymer*, 147, pp. 184-195.

Yang, M., Wang, J., Yang, Y., Zhang, Q., Ji, C., Wu, G., Su, Y., Gou, Y., Wu, Z., Yuan, K., Xiu, F. and Jiang, Y. (2019). Ultraviolet to long-wave infrared photodetectors based on a three-dimensional dirac semimetal/organic thin film heterojunction. *Journal of Physical Chemistry Letters*, 10(14), pp. 3914-3921.

Zeng, L.H., Chen, Q.M., Zhang, Z.H., Wu, D., Yuan, H., Li, Y.Y., Qarony, W., Lau, S.P., Luo, L.B. and Tsang, Y.H. (2019). Multilayered PdSe2/perovskite schottky junction for fast, self-powered, polarization-sensitive, broadband photodetectors, and image sensor application. *Advanced Science*, 6(19), 1901134.